

# Molecular modeling of 4-methylphthalonitrile for dye sensitized solar cells using quantum chemical calculations

Palanivel Senthilkumar ·  
Ponnusamy Munusamy Anbarasan

Received: 12 December 2009 / Accepted: 6 March 2010 / Published online: 2 April 2010  
© Springer-Verlag 2010

**Abstract** The geometries, electronic structures, polarizabilities, and hyperpolarizabilities of organic dye sensitizer 4-Methylphthalonitrile was studied based on Hartree-Fock (HF) and density functional theory (DFT) using the hybrid functional B3LYP. Ultraviolet-visible (UV-Vis) spectrum was investigated by time dependent-density functional theory (TD-DFT). Features of the electronic absorption spectrum in the visible and near-UV regions were assigned based on TD-DFT calculations. The absorption bands are assigned to  $\pi \rightarrow \pi^*$  transitions. Calculated results suggest that three lowest energy excited states of 4-Methylphthalonitrile are due to photo induced electron transfer processes. The interfacial electron transfer between semiconductor TiO<sub>2</sub> electrode and dye sensitizer 4-Methylphthalonitrile is due to an electron injection process from excited dye to the semiconductor's conduction band. The role of cyanine and methyl group in 4-Methylphthalonitrile in geometries, electronic structures, and spectral properties were analyzed.

**Keywords** Absorption spectrum · Density functional theory · Dye sensitizer · Electronic structure · Vibrational spectrum

## Introduction

The new technologies for direct solar energy conversion have gained more attention in the last few years. In particular, dye sensitized solar cells (DSSCs) are promising in terms of

efficiency and low cost [1–3]. The foremost feature of DSSC consists in a wide band gap nanocrystalline film grafted with a quasi-monolayer of dye molecules and submerged in a redox electrolyte. This elegant architecture can synchronously address two critical issues of employing organic materials for the photovoltaic applications: (i) efficient charge generation from the Frenkel excitons and (ii) long-lived electron-hole separation up to the millisecond time domain. The latter attribute can often confer an almost quantitative charge collection for several micrometer-thick active layers, even if the electron mobilities in nanostructured semiconducting films are significantly lower than those in the bulk crystalline materials. Benefited from systematic device engineering and continuous material innovation, a state of the art DSSC with a ruthenium sensitizer has achieved a validated efficiency of 11.1% [4] measured under the air mass 1.5 global (AM1.5G) conditions. In view of the limited ruthenium resource and the heavy-metal toxicity, metal-free organic dyes have received surging research interest in recent years [5–21]. Because of their high molar absorption coefficient, relatively simple synthesis procedure, various structures and lower cost in contrast to a ruthenium dye and the flexibility in molecular tailoring of an organic sensitizer provides a large area to explore [22–24]. Moreover, recently a rapid progress of organic dyes has been witnessed reaching close to 10.0% efficiencies in combination with a volatile acetonitrile-based electrolyte [25]. In this paper the performance of 4-Methylphthalonitrile metal free dye that can be used in DSSC is analyzed.

## Experimental details

The compound 4-Methylphthalonitrile was obtained from Sigma-Aldrich Chemical Company, USA with a stated purity of greater than 99% and it was used as such without

P. Senthilkumar (✉) · P. M. Anbarasan  
Department of Physics, Periyar University,  
Salem - 636 011,  
Tamilnadu, India  
e-mail: psenthil.vnr@gmail.com

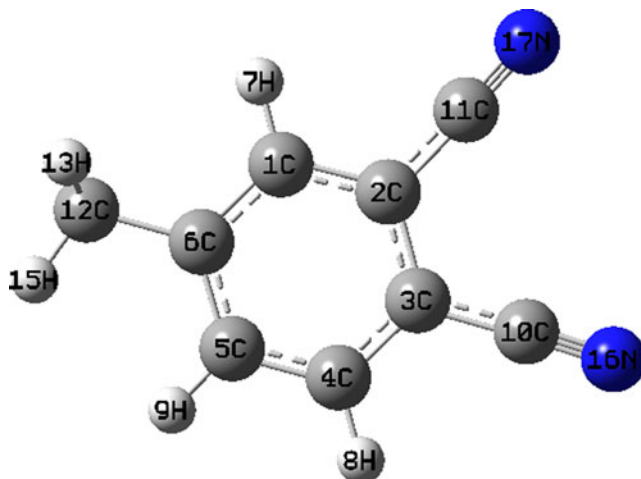


**Fig. 1** Optimized geometrical structure of dye 4-Methylphthalonitrile

further purification. The FT-Raman spectrum of 4-Methylphthalonitrile has been recorded using 1064 nm line of Nd:YAG laser as excitation wavelength in the region 50–3500 cm<sup>-1</sup> on a Brucker model IFS 66 V spectropho-

**Table 1** Bond lengths (in Å), bond angles (in degree) and dihedral angles (in degree) of the dye 4-Methylphthalonitrile

Parameters	HF/6-311G(d,p)	B3LYP/6-311G(d,p)
<b>Bond length( Å)</b>		
C1-C2	1.3824	1.3971
C1-C6	1.3913	1.3979
C1-H7	1.0746	1.0839
C2-C3	1.3972	1.4131
C2-C11	1.4425	1.4306
C3-C4	1.3832	1.3981
C3-C10	1.4408	1.4291
C4-C5	1.3845	1.3903
C4-H8	1.0737	1.0828
C5-C6	1.3859	1.3985
C5-H9	1.0749	1.0842
C6-C12	1.5087	1.5073
C10-N16	1.1297	1.1551
C11-N17	1.1295	1.1549
C12-H13	1.0854	1.0938
C12-H14	1.0854	1.0938
C12-H15	1.0828	1.0908
<b>Bond angle(°)</b>		
C2-C1-C6	121.1	121.3
C2-C1-H7	118.8	118.5
C6-C1-H7	120.0	120.0
C1-C2-C3	120.0	119.7
C1-C2-C11	118.7	119.1
C3-C2-C11	121.1	121.1
C2-C3-C4	119.1	118.9

**Table 1** (continued)

Parameters	HF/6-311G(d,p)	B3LYP/6-311G(d,p)
C2-C3-C10	121.5	121.4
C4-C3-C10	119.3	119.6
C3-C4-C5	120.3	120.4
C3-C4-H8	119.3	119.1
C5-C4-H8	120.2	120.3
C4-C5-C6	121.1	121.3
C4-C5-H9	119.0	119.1
C6-C5-H9	119.7	119.5
C1-C6-C5	118.2	118.1
C1-C6-C12	120.1	120.3
C5-C6-C12	121.6	121.4
C6-C12-H13	110.7	110.9
C6-C12-H14	110.7	110.9
C6-C12-H15	111.1	111.4
H13-C12-H14	107.7	107.2
H13-C12-H15	108.1	108.0
H13-C12-H15	108.1	108.0
<b>Dihedral angle (°)</b>		
C6-C1-C2-C3	0.0035	-0.0007
C6-C1-C2-C11	179.9	180.0
H7-C1-C2-C3	-179.9	-180.
H7-C1-C2-C11	-0.0038	0.0006
C2-C1-C6-C5	0.0027	-0.001
C2-C1-C6-C12	179.9	180.0
H7-C1-C6-C5	180.0	-180.0
H7-C1-C6-C12	-0.0051	0.0001
C1-C2-C3-C4	-0.0072	0.0018
C1-C2-C3-C10	179.9	180.0
C11-C2-C3-C4	-179.9	-179.9
C11-C2-C3-C10	0.0043	-0.0004
C2-C3-C4-C5	0.0049	-0.0011
C2-C3-C4-H8	-180.0	-180.0
C10-C3-C4-C5	-179.9	-180.0
C10-C3-C4-H8	-0.0009	-0.0001
C3-C4-C5-C6	0.0013	-0.0007
C3-C4-C5-H9	179.9	179.9
H8-C4-C5-C6	-179.9	-180.0
H8-C4-C5-H9	0.0006	-0.0003
C4-C5-C6-C1	-0.005	0.0017
C4-C5-C6-C12	-179.9	-179.9
H9-C5-C6-C1	180.0	180.0
H9-C5-C6-C12	0.0052	0.0001
C1-C6-C12-H13	-59.7	-59.5
C1-C6-C12-H14	59.7	59.5
C1-C6-C12-H15	179.9	179.9
C5-C6-C12-H13	120.2	120.4
C5-C6-C12-H14	-120.2	-120.4
C5-C6-C12-H15	-0.0087	-0.0141

tometer. The FT-IR spectrum of this compound was recorded in the region 400–4000 cm<sup>-1</sup> on IFS 66 V spectrophotometer using KBr pellet technique. The spectrum was recorded at room temperature, with scanning speed of 30 cm<sup>-1</sup> min<sup>-1</sup> and the spectral resolution of 2.0 cm<sup>-1</sup>.

## Computational methods

The computations of the geometries, electronic structures, polarizabilities and hyperpolarizabilities, as well as electronic absorption spectrum for dye sensitizer 4-Methylphthalonitrile was done using Hartree-Fock (HF) and density functional theory (DFT) with Gaussian03 package [26]. The DFT was treated according to hybrid functional Becke's three parameter gradient-corrected exchange potential and the Lee-Yang-Parr gradient-corrected correlation potential (B3LYP) [27–29], and all calculations were performed without any symmetry constraints by using polarized split-valence 6-311++G(d,p) basis sets. The NBO analysis was performed using restricted Hartree-Fock (RHF) with the same basis set. The electronic absorption spectrum requires calculation of the allowed excitations and oscillator strengths. These calculations were done using time dependent DFT (TD-DFT) with the same basis sets and exchange-correlation functional in vacuum and solution, and the non-equilibrium version of the polarizable continuum model (PCM) [30, 31] was adopted for calculating the solvent effects.

**Fig. 2** The frontier molecular orbital energies and corresponding DOS spectrum of the dye 4-Methylphthalonitrile

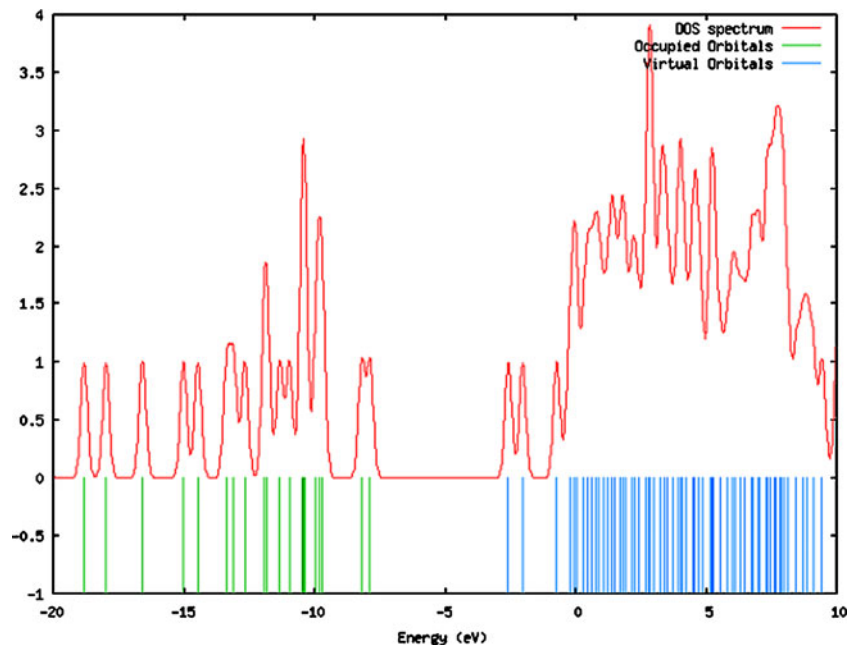
## Results and discussion

### The geometric structure

The optimized geometry of the 4-Methylphthalonitrile is shown in Fig. 1, and the bond lengths, bond angles and dihedral angles are listed in Table 1. The crystal structure of the exact title compound is not available, the optimized structure can only be compared with similar systems for which crystal structures have been solved. We can find that most of the optimized bond lengths, bond angles and dihedral angles. The distance between C2 and C3 atoms in cyanine groups of 4-Methylphthalonitrile are 1.4306 Å and 1.4291 Å respectively at B3LYP/6-311++G(d,p) and also compared with HF/6-311++G(d,p).

### Electronic structures and charges

Natural bond orbital (NBO) analysis was performed in order to analyze the charge populations of the dye 4-Methylphthalonitrile. Charge distributions in C, N and H atoms were observed because of the different electronegativity, the electrons transferred from C atoms to C, N atoms, C atoms to H and N atoms to H atom. The natural charges of different groups are the sum of every atomic natural charge in the group. These data indicate that the cyanine groups are donors and amide groups are acceptors and the charges were transferred through chemical bonds. The frontier molecular orbitals (MO) energies and corresponding density of state of the dye 4-Methylphthalonitrile is shown in Fig. 2. The HOMO–



LUMO gap of the dye 4-Methylphthalonitrile in vacuum is 5.76 eV.

While the calculated HOMO and LUMO energies of the bare  $\text{Ti}_{38}\text{O}_{76}$  cluster as a model for nanocrystalline are  $-6.55$  and  $-2.77$  eV, respectively, resulting in a HOMO–LUMO gap of 3.78 eV, the lowest transition is reduced to 3.20 eV according to TD-DFT, and this value is slightly smaller than typical band gap of  $\text{TiO}_2$  nanoparticles with nm size [32]. Furthermore, the HOMO, LUMO and HOMO-LUMO gap of  $(\text{TiO}_2)_{60}$  cluster is  $-7.52$ ,  $-2.97$ , and  $4.55$  eV (B3LYP/VDZ), respectively [33]. Taking into account the cluster size effects and the calculated HOMO, LUMO, HOMO–LUMO gap of the dye 4-Methylphthalonitrile,  $\text{Ti}_{38}\text{O}_{76}$  and  $(\text{TiO}_2)_{60}$  clusters, we can find that the HOMO energies of these dyes fall within the  $\text{TiO}_2$  gap.

The above data also reveal the interfacial electron transfer between semiconductor  $\text{TiO}_2$  electrode and the dye sensitizer 4-Methylphthalonitrile is electron injection processes from excited dye to the semiconductor conduction band. This is a kind of typical interfacial electron transfer reaction [34].

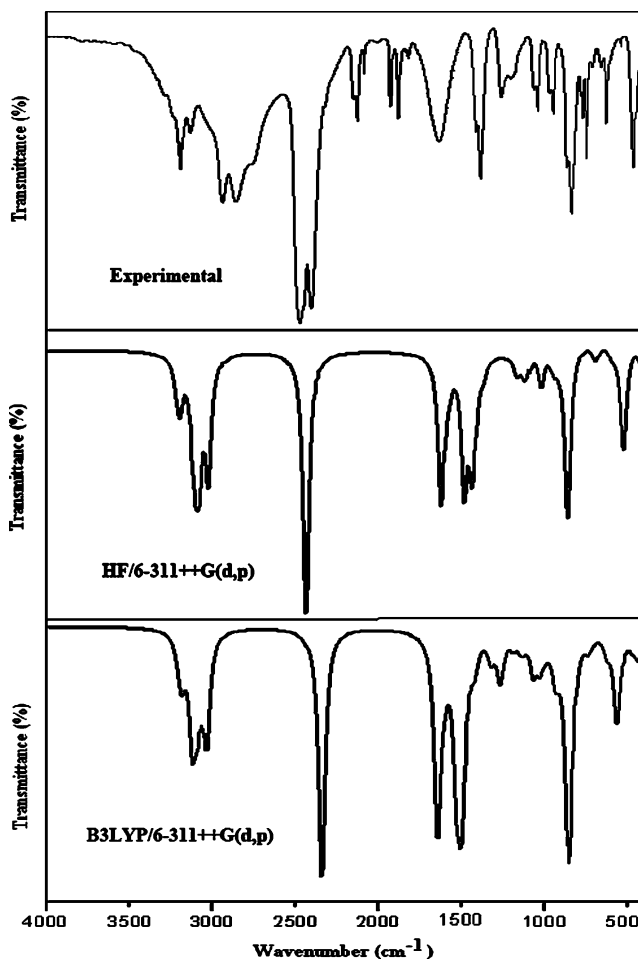


**Fig. 3** Observed and calculated FT-IR spectra of the dye 4-Methylphthalonitrile

## IR and Raman frequencies

Figures 3 and 4 shows the observed and calculated IR and Raman spectra of 4-Methylphthalonitrile respectively. Comparison of the observed (FT-IR and FT-Raman) and calculated vibrational frequencies of 4-Methylphthalonitrile is shown in Table 2. Comparison of the frequencies calculated by HF and B3LYP with experimental values reveals the overestimation of the calculated vibrational modes due to neglect of anharmonicity. A corrective vibrational scaling factor of 0.9613 to B3LYP calculated frequencies and scaling factor of 0.8982 to HF calculated frequencies were applied to account for anharmonicity. Inclusion of electron correlation in density functional theory to a certain extent makes the frequency values

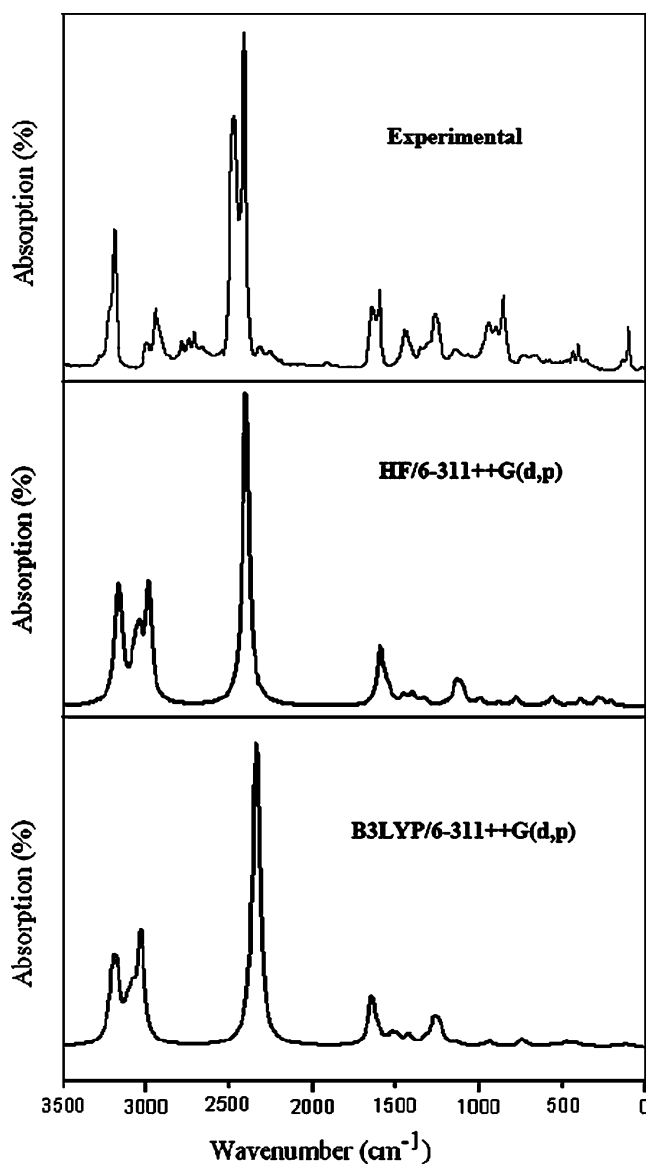


**Fig. 4** Observed and calculated FT-Raman spectra of the dye 4-Methylphthalonitrile

**Table 2** Comparison of the observed (FT-IR and FT-Raman) and calculated vibrational frequencies of 4-Methylphthalonitrile

Vibrational mode no.	Species	Experimental		Scaled wavenumber ( $\text{cm}^{-1}$ )		IR intensity	Raman active	Assignments
		FT-IR	FT-Raman	HF/6-311++G (d,p)	B3LYP/6-311++G (d,p)			
1	A''	—	—	−15	−56	0.25	0.43	$\gamma$ C-C-N
2	A'	—	—	105	95	0.83	0.59	$\beta$ C-C-N
3	A'	—	—	131	118	1.58	6.51	$\beta$ C-C-N
4	A'	—	—	154	139	1.76	0.35	$\beta$ C-C-N
5	A'	—	—	188	172	4.43	0.63	$\beta$ C-C-N
6	A'	—	—	274	250	4.24	0.10	$\beta$ C-C-N
7	A''	—	—	364	340	1.76	0.63	$\gamma$ C-C-N
8	A''	—	—	428	389	0.54	1.31	$\tau$ C-C-C
9	A'	—	—	429	402	0.29	5.44	$\delta$ C-C-C
10	A'	—	—	477	434	2.87	1.84	$\delta$ C-C-C
11	A'	—	487	499	466	1.24	13.34	$\delta$ C-C-C
12	A'	—	—	588	539	0.35	2.52	$\beta$ C-C-N
13	A''	579	—	612	556	11.99	3.14	$\gamma$ C-C-N + $\gamma$ C-H
14	A'	—	—	670	617	2.01	0.85	$\beta$ C-C-N
15	A'	—	—	690	637	0.04	0.81	$\beta$ C-C-N
16	A''	—	—	754	710	0.47	2.57	$\tau$ C-C-N + $\omega$ C-H
17	A''	—	765	778	732	1.53	18.09	$\omega$ C-C-N + $\omega$ C-H
18	A'	—	—	824	755	0.001	0.84	$\omega$ C-H
19	A''	988	—	939	846	31.07	0.23	$\omega$ C-H
20	A''	—	—	991	920	3.49	0.33	$\omega$ C-H
21	A'	—	971	1023	934	2.12	14.78	$\omega$ C -H
22	A''	—	—	1092	988	1.33	0.05	$\omega$ C-H
23	A'	—	—	1101	1023	3.65	1.42	$\beta$ C-H
24	A'	1095	—	1165	1063	4.72	0.06	$\beta$ C-H
25	A'	—	1162	1200	1129	2.02	8.47	$\beta$ C-H
26	A'	—	—	1221	1178	1.49	1.34	$\beta$ C-H
27	A'	—	1244	1297	1230	0.42	36.48	$\nu$ C=C
28	A'	1287	1271	1317	1260	6.07	70.83	$\nu$ C=C
29	A'	—	—	1349	1307	0.59	5.88	$\nu$ C=C
30	A'	—	1333	1410	1318	2.42	11.14	$\nu$ C=C + $\nu$ C-C-N
31	A'	—	1428	1537	1416	2.53	25.32	$\nu$ C=C
32	A'	—	—	1549	1429	0.85	4.16	$\nu$ C=C
33	A'	1504	1511	1604	1485	8.90	10.32	$\nu$ C=C
34	A'	1556	1548	1613	1494	13.31	10.03	$\nu$ C=C
35	A'	1582	1559	1659	1522	16.02	22.77	$\nu$ C=C
36	A'	—	1605	1749	1595	3.13	25.14	$\nu$ C=C
37	A'	1678	1652	1794	1639	26.65	135.46	$\nu$ C=C
38	A'	—	2341	2595	2337	23.37	589.10	$\nu$ C-N
39	A'	2346	2346	2597	2339	10.55	290.82	$\nu$ C-N
40	A'	3042	3056	3175	3031	13.91	307.52	$\nu$ C-H
41	A'	3095	3104	3230	3083	8.39	93.75	$\nu$ C-H
42	A'	3139	3164	3257	3114	12.78	67.45	$\nu$ C-H
43	A'	—	3193	3340	3177	4.88	86.00	$\nu$ C-H
44	A'	—	3207	3348	3184	1.18	65.41	$\nu$ C-H
45	A'	—	3256	3365	3201	1.28	134.48	$\nu$ C-H

$\nu$  - stretching;  $\nu_{\text{sym}}$ -symmetric stretching ;  $\nu_{\text{asy}}$ -asymmetric stretching; Rb-Ring breathing;  $\beta$ -in plane bending;  $\gamma$ - out-of-plane bending;  $\omega$ -wagging;  $\tau$ - torsion ;  $\delta$ - ring deformation

**Table 3** Polarizability ( $\alpha$ ) of the dye 4-Methylphthalonitrile (in a.u.)

$\alpha_{xx}$	$\alpha_{xy}$	$\alpha_{yy}$	$\alpha_{xz}$	$\alpha_{yz}$	$\alpha_{zz}$	$\alpha$	$\Delta\alpha$
162.089	2.054	122.631	0.092	0.022	60.695	115.138	88.526

smaller in comparison to experimental values. Any way notwithstanding the level of calculations it is customary to scale down the calculated harmonic frequencies in order to improve the agreement with the experiment. In our study we have followed two different scaling factors B3LYP/6-311++G(d,p) and HF/6-311++G(d,p). The 4-Methylphthalonitrile molecule gives rise to six C-H stretching, eight C-H wagging vibrations, four C-H in-plane bending vibration, seven wagging C-C-N vibrations, one C-C-N stretching vibration, one C-C-N torsion vibration, 11 C=C stretching vibrations, two C-N stretching vibrations, six C-H stretching vibrations, four C-H in plane bending vibrations, eight C-H wagging vibrations, three ring deformation vibrations and one ring torsion vibrations were assigned. The strongest IR absorption for 4-Methylphthalonitrile corresponds to the vibrational mode 19 near about  $846\text{ cm}^{-1}$ , which is the ring breathing mode of C-C bonds. The next stronger IR absorption is attributed to vibrational mode 37 near about  $1639\text{ cm}^{-1}$ , corresponding to stretching mode of C=C bonds. In the Raman spectra, however, the strongest activity mode is the vibrational mode 38 near about  $2337\text{ cm}^{-1}$ , which is corresponding to stretching mode of C-N triple bond.

#### Polarizability and hyperpolarizability

Polarizabilities and hyperpolarizabilities characterize the response of a system in an applied electric field [35]. They determine not only the strength of molecular interactions (long-range intermolecular induction, dispersion forces, etc.) as well as the cross sections of different scattering and collision processes, but also the nonlinear optical properties (NLO) of the system [36, 37]. It has been found that the dye sensitizer hemicyanine system, which has high NLO property, usually possesses high photoelectric conversion performance [38]. In order to investigate the relationships among photocurrent generation, molecular structures and NLO, the polarizabilities and hyperpolarizabilities of 4-Methylphthalonitrile was calculated.

The polarizabilities and hyperpolarizabilities could be computed *via* finite field (FF) method, sum-over state (SOS) method based on TD-DFT, and coupled-perturbed HF (CPHF) method. However, the use of FF, SOS, and

CPHF methods with large sized basis sets for 4-Methylphthalonitrile is too expensive. Here, the polarizability and the first hyperpolarizabilities are computed as a numerical derivative of the dipole moment using B3LYP/6-311++G(d,p). The definitions [36, 37] for the isotropic polarizability is

$$\alpha = \frac{1}{3}(\alpha_{XX} + \alpha_{YY} + \alpha_{ZZ}). \quad (1)$$

The polarizability anisotropy invariant is

$$\Delta\alpha = \left[ \frac{(\alpha_{XX} - \alpha_{YY})^2 + (\alpha_{YY} - \alpha_{ZZ})^2 + (\alpha_{ZZ} - \alpha_{XX})^2}{2} \right]^{\frac{1}{2}}, \quad (2)$$

and the average hyperpolarizability is

$$\beta_{||} = \frac{1}{5}(\beta_{iiz} + \beta_{izi} + \beta_{Zii}). \quad (3)$$

Where,  $\alpha_{XX}$ ,  $\alpha_{YY}$  and  $\alpha_{ZZ}$  are tensor components of polarizability;  $\beta_{iiz}$ ,  $\beta_{izi}$ , and  $\beta_{Zii}$  (i from X to Z) are tensor components of hyperpolarizability.

Tables 3 and 4 list the values of the polarizabilities and hyperpolarizabilities of the dye 4-Methylphthalonitrile. In addition to the individual tensor components of the polarizabilities and the first hyperpolarizabilities, the isotropic polarizability, polarizability anisotropy invariant and hyperpolarizability are also calculated. The calculated isotropic polarizability of 4-Methylphthalonitrile is 115.138 a.u. However, the calculated isotropic polarizabilities of JK16, JK17, dye 1, dye 2, D5, DST and DSS are 759.9, 1015.5, 694.7, 785.7, 510.6, 611.2 and 802.9 a.u., respectively [39, 40]. The above data indicate that the donor-conjugate pi bridge-acceptor (D-pi-A) chain-like dyes have stronger response for external electric field. Whereas, for dye sensitizers D5, DST, DSS, JK16, JK17, dye 1 and dye 2, on the basis of the published photo-to-current conversion efficiencies, the similarity and the difference of geometries, and the calculated isotropic polarizabilities, it is found that the longer the length of the conjugate bridge in similar dyes, the larger the polarizability of the dye molecule, and the lower the photo-to-current conversion efficiency. This may be due to the fact that the longer conjugate-p-bridge enlarged the delocalization of electrons, thus it enhanced the response of the external field, but the enlarged delocalization may not be favorable to generate charge separated state effectively. So it induces the lower photo-to-current conversion efficiency.

**Table 4** Hyperpolarizability ( $\beta$ ) of the dye 4-Methylphthalonitrile (in a.u.)

$\beta_{xxx}$	$\beta_{xxy}$	$\beta_{xyy}$	$\beta_{yyy}$	$\beta_{xxz}$	$\beta_{xyz}$	$\beta_{yyz}$	$\beta_{xzz}$	$\beta_{yzz}$	$\beta_{zzz}$	$\beta_{ii}$
-99.4195	4.7561	-41.448	-31.484	1.6886	-0.090	0.764	-0.466	2.165	0.6522	1.86216

## Electronic absorption spectra and sensitized mechanism

The UV-Vis spectra of 4-Methylphthalonitrile were measured in acetonitrile solution, and it is found that the absorption bands centered at 202 and 224 nm in UV region, respectively. Electronic absorption spectra of 4-Methylphthalonitrile in vacuum and solvent were performed using TD-DFT (B3LYP)/6-311++G(d,p) calculations, and the results are shown in Fig. 5. It is observed that the absorption in the visible region is much weaker than that in the UV region for 4-Methylphthalonitrile. The results of TD-DFT have an appreciable red-shift in vacuum and solvent, and the degree of red-shift in solvent is more significant than that in vacuum. The discrepancy between vacuum and solvent effects in TD-DFT calculations may result from two aspects. The first aspect is a smaller gap of materials which induces smaller excited energies. The other is solvent effects. Experimental measurements of electronic absorptions are usually performed in solution. Solvent, especially polar solvent, could affect the geometry and electronic structure as well as the properties of molecules through the long-range interaction between solute molecule and solvent molecule. For these reasons it is more difficult to make the TD-DFT calculation consistent with quantitatively. Though the discrepancy exists, the TD-DFT calculations are capable of describing the spectral features of 4-Methylphthalonitrile because of the agreement of line shape and relative strength as compared with the vacuum and solvent.

The HOMO-LUMO gap of 4-Methylphthalonitrile in acetonitrile at B3LYP/6-311++G (d,p) theory level is smaller than that in vacuum. This fact indicates that the solvent effects stabilize the frontier orbitals of 4-Methylphthalonitrile. So it induces the smaller intensities

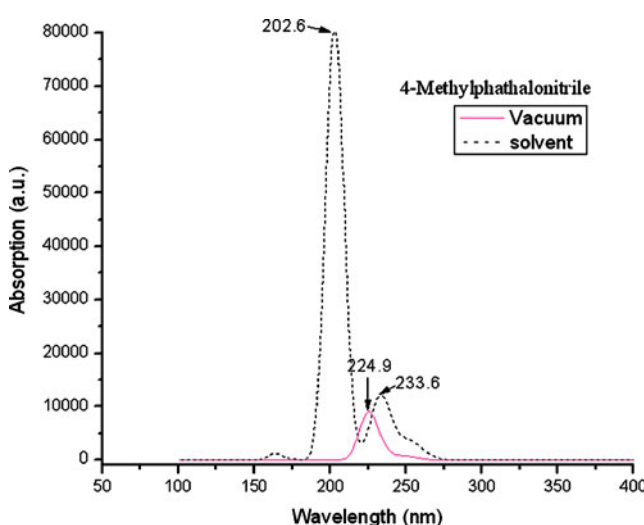


**Fig. 5** Calculated electronic absorption spectra of the dye 4-Methylphthalonitrile

and red-shift of the absorption as compared with that in vacuum.

In order to obtain the microscopic information about the electronic transitions, the corresponding MO properties are checked. The absorption in visible and near-UV region is the most important region for photo-to-current conversion, so only the 20 lowest singlet/singlet transitions of the absorption band in visible and near-UV region for 4-Methylphthalonitrile is listed in Table 5. The data of Table 5 and Fig. 6 are based on the 6-311++G(d,p) results with solvent effects involved.

This indicates that the transitions are photoinduced charge transfer processes, thus the excitations generate charge separated states, which should favor the electron injection from the excited dye to semiconductor surface.

The solar energy to electricity conversion efficiency ( $\eta$ ) under AM 1.5 white-light irradiation can be obtained from the following formula:

$$\eta(\%) = \frac{J_{SC}[mAcm^{-2}]V_{OC}[V]ff}{I_0[mWcm^{-2}]} \times 100, \quad (4)$$

Where  $I_0$  is the photon flux,  $J_{sc}$  is the short-circuit photocurrent density, and  $V_{oc}$  is the open-circuit photovoltage, and  $ff$  represents the fill factor [41]. At present, the  $J_{sc}$ , the  $V_{oc}$ , and the  $ff$  are only obtained by experiment, the relationship among these quantities and the electronic structure of dye is still unknown. The analytical relationship between  $V_{oc}$  and  $E_{LUMO}$  may exist. According to the sensitized mechanism (electron injected from the excited dyes to the semiconductor conduction band) and single electron and single state approximation, there is an energy relationship:

$$eV_{oc} = E_{LUMO} - E_{CB}. \quad (5)$$

Where,  $E_{CB}$  is the energy of the semiconductor's conduction band edge. So the  $V_{oc}$  may be obtained applying the following formula:

$$V_{oc} = \frac{(E_{LUMO} - E_{CB})}{e}. \quad (6)$$

It induces that the higher the  $E_{LUMO}$ , the larger the  $V_{oc}$ . The results of organic dye sensitizer JK16 and JK17 [39], D-ST and D-SS also proved the tendency [42] (JK16: LUMO=−2.73 eV,  $V_{oc}=0.74$  V; JK17: LUMO=−2.87 eV,  $V_{oc}=0.67$  V; D-SS: LUMO=−2.91 eV,  $V_{oc}=0.70$  V; D-ST: LUMO=−2.83 eV,  $V_{oc}=0.73$  V). Certainly, this formula expects further test by experiment and theoretical calculation. The  $J_{sc}$  is determined by two processes, one is the rate of electron injection from the excited dyes to the conduction band of semiconductor, and the other is the rate of redox between the excited dyes and electrolyte. Electrolyte effect on the redox processes is very complex, and it is not

**Table 5** Computed excitation energies, electronic transition configurations and oscillator strengths (f) for the optical transitions with  $f > 0.01$  of the absorption bands in visible and near-UV region for the dye 4-Methylphthalonitrile in acetonitrile

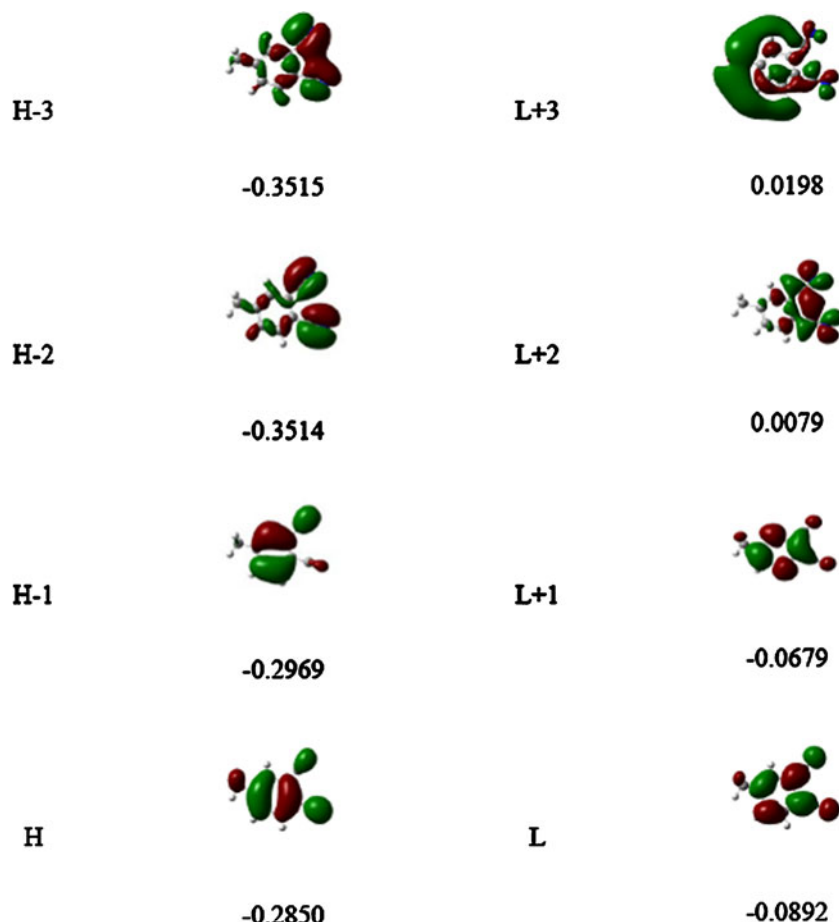
State	Configurations composition (corresponding transition orbitals)	Excitation energy (eV/nm)	Oscillator strength (f)
1	-0.36991 (36→38) -0.26097 (36→39) 0.44484 (37→38) -0.30891 (37→39)	4.9113 / 252.45	0.0455
2	0.41420 (36→38) -0.11709 (36→39) 0.43248 (37→38) 0.26844 (37→39)	5.3214 / 232.99	0.1650
3	-0.35001 (36→38) 0.50369 (37→39)	6.0656 / 204.41	0.8428
4	0.58300 (36→39) 0.19976 (37→38) -0.10214 (37→39)	6.2405 / 198.68	0.4329

taken into account in the present calculations. This indicates that most of the excited states of 4-Methylphthalonitrile have a larger absorption coefficient, and then with a shorter lifetime for the excited states, so it results in the higher electron injection rate which leads to the larger  $J_{sc}$  of 4-Methylphthalonitrile. On the basis of above analysis, it is clear that the 4-Methylphthalonitrile has better performance in DSSC.

## Conclusions

The geometries, electronic structures, polarizabilities, and hyperpolarizabilities of dye 4-Methylphthalonitrile was studied by using HF and DFT with hybrid functional B3LYP, and the UV-Vis spectra were investigated by using TD-DFT methods. The NBO results suggest that 4-Methylphthalonitrile is a (D-pi-A) system. The calculated

**Fig. 6** Isodensity plots (isodensity contour = 0.02 a.u.) of the frontier orbitals of dye 4-Methylphthalonitrile and corresponding orbital energies (eV)



isotropic polarizability of 4-Methylphthalonitrile is 115.138 a.u. The calculated polarizability anisotropy invariant of 4-Methylphthalonitrile is 88.526 a.u. The hyperpolarizability of 4-Methylphthalonitrile is 1.8621 (in a.u). The strongest IR absorption for 4-Methylphthalonitrile corresponds to the vibrational mode 19 near about 846 cm<sup>-1</sup>, which is the ring breathing mode of C-C bonds. The next stronger IR absorption is attributed to vibrational mode 37 near about 1639 cm<sup>-1</sup>, corresponding to the stretching mode of C=C bonds. In the Raman spectra, however, the strongest activity mode is the vibrational mode 38 near about 2337 cm<sup>-1</sup>, which is corresponding to the stretching mode of C-N triple bond. The electronic absorption spectral features in visible and near-UV region were assigned based on the qualitative agreement to TD-DFT calculations. The absorptions are all ascribed to  $\pi \rightarrow \pi^*$  transition. The three excited states with the lowest excited energies of 4-Methylphthalonitrile are photoinduced electron transfer processes that contribute sensitization of photo-to-current conversion processes. The interfacial electron transfer between semiconductor TiO<sub>2</sub> electrode and dye sensitizer 4-Methylphthalonitrile is electron injection process from excited dye as donor to the semiconductor conduction band. Based on the analysis of geometries, electronic structures, and spectrum properties of 4-Methylphthalonitrile, the role of cyanine and amine group in phthalonitrile is as follows: it enlarged the distance between electron donor group and semiconductor surface, and decreased the timescale of the electron injection rate, resulting in giving lower conversion efficiency. This indicates that the choice of the appropriate conjugate bridge in dye sensitizer is very important to improve the performance of DSSC.

**Acknowledgments** This work was partly financially supported by University Grants Commission, Govt. of India, New Delhi, within the Major Research Project scheme under the approval-cum-sanction No. F.No.34-5/2008(SR) & 34-1/TN/08.

## References

- O'Regan B, Gratzel M (1991) Nature 353:737–739
- Gratzel M (2001) Nature 414:338–344
- Park NG, Kim K (2008) Phys Stat Sol a 205:1895–1904
- Chiba Y, Islam A, Watanabe Y, Komiya R, Koide N, Han L (2006) J Appl Phys 45:L638–L640
- Hara K, Kurashige M, Dan-oh Y, Kasada C, Shinpo A, Suga S, Sayama K, Arakawa H (2003) New J Chem 27:783–785
- Kitamura T, Ikeda M, Shigaki K, Inoue T, Anderson NA, Ai X, Lian T, Yanagida S (2004) Chem Mater 16:1806–1812
- Horiuchi T, Miura H, Sumioka K, Uchida S (2004) J Am Chem Soc 126:12218–12219
- Campbell WM, Burrell AK, Officer DL, Jolley KW (2004) Coord Chem Rev 248:1363–1379
- Thomas KRJ, Lin JT, Hsu YC, Ho KC (2005) Chem Commun 4098–4100
- Hagberg DP, Edvinsson T, Marinado T, Boschloo G, Hagfeldt A, Sun L (2006) Chem Commun 2245–2247
- Li SL, Jiang KJ, Shao KF, Yang LM (2006) Chem Commun 2792–2794
- Koumura N, Wang ZS, Mori S, Miyashita M, Suzuki E, Hara K (2006) J Am Chem Soc 128:14256–14257
- Kim S, Lee JW, Kang SO, Ko J, Yum JH, Fantacci S, De Angelis F, Di Censo D, Nazeeruddin MK, Gratzel MJ (2006) J Am Chem Soc 128:16701–16707
- Wang ZS, Cui Y, Hara K, Dan-oh Y, Kasada C, Shinpo A (2007) Adv Mater 19:1138–1141
- Edvinsson T, Li C, Pschirer N, Schoneboom J, Eickemeyer F, Sens R, Boschloo G, Herrmann A, Mullen K, Hagfeldt A (2007) J Phys Chem C 111:15137–15140
- Wang M, Xu M, Shi D, Li R, Gao F, Zhang G, Yi Z, Humphry-Baker R, Wang P, Zakeeruddin SM, Gratzel M (2008) Adv Mater 20:4460–4463
- Shi D, Pootrakuchote N, Yi Z, Xu M, Zakeeruddin SM, Gratzel M, Wang PJ (2008) J Phys Chem C 112:17478–17484
- Zhou G, Pschirer N, Schoneboom JC, Eickemeyer F, Baumgarten M, Mullen K (2008) Chem Mater 20:1808–181
- Lin JT, Chen PC, Yen YS, Hsu YC, Chou HH, Yeh MCP (2009) Org Lett 11:97–100
- Zhang G, Bai Y, Li R, Shi D, Wenger S, Zakeeruddin SM, Gratzel M, Wang P (2009) Energy Environ Sci 2:92–95
- Xu M, Wenger S, Bara H, Shi D, Li R, Zhou Y, Zakeeruddin SM, Gratzel M, Wang P (2009) J Phys Chem C 113:2966–2973
- Zhang XH, Li C, Wang WB, Cheng XX, Wang XS, Zhang BW (2007) J Mater Chem 17:642–649
- Liang M, Xu W, Cai F, Chen P, Peng B, Chen J, Li Z (2007) J Phys Chem C 111:4465–4472
- Xu W, Peng B, Chen J, Liang M, Cai F (2008) J Phys Chem C 112:874–880
- Ito S, Miura H, Uchida S, Takata M, Sumioka K, Liska P, Comte P, Pechy P, Gratzel M (2008) Chem Commun 5194–5196
- Frisch MJ, Trucks GW, Schlegel HB, Scuseria GE, Robb MA, Cheeseman JR, Montgomery JA Jr, Vreven T, Kudin KN, Burant JC, Millam JM, Iyengar SS, Tomasi J, Barone V, Mennucci B, Cossi M, Scalmani G, Rega N, Petersson GA, Nakatsuji H, Hada M, Ehara M, Toyota K, Fukuda R, Hasegawa J, Ishida M, Nakajima T, Honda Y, Kitao O, Nakai H, Klene M, Li X, Knox JE, Hratchian HP, Cross JB, Adamo C, Jaramillo J, Gomperts R, Stratmann RE, Yazyev O, Austin AJ, Cammi R, Pomelli C, Ochterski JW, Ayala PY, Morokuma K, Voth GA, Salvador P, Dannenberg JJ, Zakrzewski VG, Dapprich S, Daniels AD, Strain MC, Farkas O, Malick DK, Rabuck AD, Raghavachari K, Foresman JB, Ortiz JV, Cui Q, Baboul AG, Clifford S, Cioslowski J, Stefanov BB, Liu G, Liashenko A, Piskorz P, Komaromi I, Martin RL, Fox DJ, Keith T, Al-Laham MA, Peng CY, Nanayakkara A, Challacombe M, Gill PMW, Johnson B, Chen W, Wong MW, Gonzalez C, Pople JA (2003) Gaussian 03. Gaussian Inc, Pittsburgh
- Becke AD (1993) J Chem Phys 98:5648–5652
- Miehlich B, Savin A, Stoll H, Preuss H (1989) Chem Phys Lett 157:200–206
- Lee C, Yang W, Parr RG (1988) Phys Rev B 37:785–789
- Barone V, Cossi M (1998) J Phys Chem A 102:1995–2001
- Cossi M, Rega N, Scalmani G, Barone V (2003) J Comput Chem 24:669–681
- Nazeeruddin MK, De Angelis F, Fantacci S, Selloni A, Viscardi G, Liska P, Ito S, Takeru B, Gratzel M (2005) J Am Chem Soc 127:16835–16847
- Lundqvist MJ, Nilsing M, Persson P, Lunell S (2006) Int J Quantum Chem 106:3214–3234

34. Waston DF, Meyer GJ (2005) *Annu Rev Phys Chem* 56:119–156
35. Zhang CR, Chen HS, Wang GH (2004) *Chem Res Chin U* 20:640–646
36. Sun Y, Chen X, Sun L, Guo X, Lu W (2003) *Chem Phys Lett* 381:397–403
37. Christiansen O, Gauss J, Stanton JF (1999) *Chem Phys Lett* 305:147–155
38. Wang ZS, Huang YY, Huang CH, Zheng J, Cheng HM, Tian SJ (2000) *Synth Met* 14:201–207
39. Zhang CR, Wu YZ, Chen YH, Chen HS (2009) *Acta Phys Chim Sin* 25:53–60
40. Seidl GA, Vogl P, Majewski JA, Levy M (1996) *Phys Rev B* 53:3764–3774
41. Hara K, Sato T, Katoh R, Furube A, Ohga Y, Shinpo A, Suga S, Sayama K, Sugihara H, Arakawa H (2003) *J Phys Chem B* 107:597–606
42. Zhang CR, Liu ZJ, Chen YH, Chen HS, Wu YZ, Yuan LH (2009) *J Mol Struct THEOCHEM* 899:86–93